Journal of Environmental Management 351 (2024) 119719

Contents lists available at ScienceDirect

Journal of Environmental Management

journal homepage: www.elsevier.com/locate/jenvman

Research article

Using landfill leachate to indicate the chemical and biochemical activities in elevated temperature landfills

Synthia P. Mallick [a,1], Harsh V. Patel [b,1], Sailee Gawande [c], Alfred Wadee [d], Huan Chen [e], Amy M. McKenna [e,h], Brian Brazil [f], Wenzheng Yu [g], Renzun Zhao [b,*]

[a] Black & Veatch, Tampa, FL, 33607, USA
[b] Department of Civil, Architectural and Environmental Engineering, North Carolina A&T State University, Greensboro, NC, 27411, USA
[c] Texas Commission on Environmental Quality (TCEQ), Fort Worth, TX, 76118, USA
[d] HDR, Inc. Raleigh, NC, 27601, USA
[e] National High Magnetic Field Laboratory, 1800 East Paul Dirac Drive, Tallahassee, FL, 32310-4205, USA
[f] Waste Management Inc. Gaithersburg, MD, 20878, USA
[g] State Key Laboratory of Environmental Aquatic Chemistry, Key Laboratory of Drinking Water Science and Technology, Research Center for Eco-Environmental Sciences, Chinese Academy of Sciences, Beijing, 100085, China
[h] Department of Soil and Crop Sciences, Colorado State University, Fort Collins, CO, USA

ARTICLE INFO

Handling Editor: Lixiao Zhang

Keywords:
Elevated temperature landfill (ETLF)
Landfill leachate
Fourier-transform ion cyclotron resonance mass spectrometry (FT-ICRMS)
DOM
Humic substance (HS)
Volatile fatty acids (VFA)

ABSTRACT

Landfill leachate properties contain important information and can be a unique indicator for the chemical and biochemical activities in landfills. In the recent decade, more landfills are experiencing elevated temperature, causing an imbalance in the decomposition of solid waste and affecting the properties of the landfill leachate. This study analyzes the properties of leachate from two landfills that were experiencing elevated temperature (ETLFs), samples were collected from both elevated temperature impacted and non-impacted areas in each landfill. The accumulation of volatile fatty acids (VFA) in leachates from elevated temperature impacted areas of both landfill sites revealed that methanogenesis was inhibited by the elevated temperature, which was further confirmed by the more acidic pH, higher H/C elemental ratio, and lower degree of aromaticity of the elevated temperature impacted leachates. Also, carbohydrates depletion indicated possible enhancement of hydrolysis and acidogenesis by elevated temperature, which was supported by compositional comparison of isolated acidic species by negative-ion electrospray ionization (ESI) Fourier transform ion cyclotron resonance mass spectrometry (FT-ICRMS) at 21 T derived from both elevated temperature impacted and non-impacted areas in the same landfill site. Furthermore, leachate organics fractionation showed that leachates not impacted by elevated temperature contain less hydrophilic fraction and more humic fraction than elevated temperature-impacted leachates for both ETLFs.

1. Introduction

Generation of municipal solid waste (MSW) is increasing each year with more population. In 2018, a total of 292.2 million tons of MSW were generated in the United States, of which 146.12 million tons were landfilled (US EPA, 2020). Moisture coming from the degraded wastes form leachates by mixing with percolated rainwater (Iskander et al., 2017). Landfills produce leachates throughout the working life and continue to do so even decades after the landfills are decommissioned (Yu, 2013). Typically, leachates have high ammonia concentration, medium or low BOD_5/COD ratio, high concentration of heavy metals and bio-refractory materials (Deng and Englehardt, 2006; Yuan et al., 2016; Zhang et al., 2013). Leachates may percolate and contaminate groundwater and soil if not managed properly (El-Fadel et al., 1997). Leachate management is, therefore, one of the major concerns for landfill operation.

The waste disposed of in landfills undergoes several physicochemical and biological processes, including hydrolysis, acidogenesis, acetogenesis, methanogenesis, etc. During each process, the waste undergoes decomposition, simultaneously generating leachate. Hence, the physio-

* Corresponding author.
E-mail address: rzhao@ncat.edu (R. Zhao).
[1] These authors equally contributed to this work.

https://doi.org/10.1016/j.jenvman.2023.119719
Received 10 September 2023; Received in revised form 5 November 2023; Accepted 23 November 2023
Available online 2 December 2023

bio-chemical processes of waste decomposition in landfills have a causal influence on leachate characteristics. For example, leachate generated during hydrolysis process of waste decomposition, should contain hydrolysis products such as carbohydrates, amino acids, fatty acids, etc., while the leachate generated during the initial stages of waste disposal should contain more organic polymers such as lignin, lipids, proteins, polysaccharides, etc. Studies track landfill leachate characteristics with each phase of decomposition show that leachate generated during acid formation phase has lower pH and higher organic matter concentration COD (1,500 to 71,100 mg L^{-1}) (Adhikari et al., 2014; Mor et al., 2006), while leachate generated after stable methanogenesis may have higher BOD_5/COD ratio influencing the biodegradability of the leachate (Cossu et al., 1998; Ehrig, 1989). Hence, it is clear leachate characteristics has a direct correlation with biochemical activities in landfill waste decomposition.

Fourier transform ion cyclotron resonance mass spectrometry (FT-ICR MS) has been widely applied to speciate organic molecules in aqueous systems, including natural organic matter (Schmidt et al., 2011; Kellerman et al., 2014), wastewater treatment effluents, stormwater runoff (Wen et al., 2020), water impacted by oil contaminants, drinking water (Hou et al., 2022), flowback water from hydraulic fracking (Liberatore et al., 2020), glacial waters (Dubnick, et al., 2022), biochar (McKenna et al., 2021), wildfire-impacted waters (Roth et al., 2022) and detection of novel and emerging contaminants (Young et al., 2022). The polyfunctionality and polydispersity in composition, molecular weight, and structure challenge nearly all other mass analyzers that cannot achieve resolving power sufficient to separate the tens of thousands of molecules that differ in mass by less than the mass of an electron. Only 21 T FT-ICR MS can routinely achieve resolving power in excess of 1, 500,000–2,000,000 that enables resolution and accurate elemental composition assignments across a wide molecular weight range ($150 < m/z < 1200$) with sub-ppm mass accuracy (Hendrickson et al., 2015). Negative-ion electrospray ionization is widely applied to aqueous samples after solid phase extraction (Dittmar et al., 2008) to preconcentration the organic carbon extracts to selectively deprotonate acidic species that can be detected by FT-ICR MS at 21 T, the highest resolving, highest sensitivity mass analyzer to date (Bahureksa et al., 2022; Smith et al., 2018).

Elevated temperature landfills (ETLF) are municipal solid waste landfills that exhibit temperatures above regulatory thresholds (145 °F, 62 °C) due to abnormal chemical reactions within the waste mass. Elevated temperature of the landfill influences engineering response and decomposition of wastes (Hanson et al., 2013). Typically, landfills operate at 30–60 °C whereas some landfills experience elevated temperature at the range of 80–100 °C (Hao et al., 2017; Narode et al., 2021). Generally, the optimum temperature for methanogenic activities is approximately 47.5–57.5 °C while 37, 75, and 95% of decrease in methanogenic activities was observed at approximately 62.5, 67.5, and 72 °C (De la Cruz et al., 2021; Schupp et al., 2021). Also, hyperthermophilic (>65 °C) conditions improve the hydrolysis and acidogenesis process compared to mesophilic conditions (25–45 °C) (Fang et al., 2020; Lee et al., 2014; Yuan et al., 2019). Previous studies show elevated temperature can impact the landfill gas, proving that the methane generation can decrease significantly due to elevated temperatures in the landfill cells (Hartz et al., 1982; Jafari et al., 2017a, 2017b; Martin et al., 2013; Schupp et al., 2021; Stark et al., 2012). However, very limited studies have been conducted on landfill leachate under elevated temperature. Hence, elevated temperature in the range of 80–100 °C can have a significant impact on the leachate composition, which frames the hypothesis and aim of this study to use landfill leachate characteristics to explain associative chemical and biochemical activities occurring in the landfills.

2. Materials and methods

2.1. Leachate sample

Leachate samples were collected from two landfills, site-A and site-B, from Virginia and Ohio, respectively. For each site, leachates were collected from two locations, i.e., impacted and not impacted by elevated temperature, termed as impacted leachate and non-impacted leachate, respectively. The leachate collection system is designed with a minimum 2 % slope to drain to collection sumps. At each sampling location, multiple leachate samples were collected by a leachate collection sump consists of an HDPE riser and submersible pump. Leachate samples were collected and sent by the landfill operators in sealed 19-liter opaque containers. The samples were stored at 4 °C and shaken well to get a homogenous mixture before each test.

2.2. Analytical measurements

Analytical measurements performed for raw landfill leachates included total organic carbon (TOC), chemical oxygen demand (COD), biochemical oxygen demand (BOD_5), UV_{254} absorbance, total solids (TS), total suspended solids (TSS) tests. For TOC and UV absorbance at 254 nm (UV_{254} absorbance) and 280 nm (e_{280}), Teledyne Tekmar (Mason, OH, USA) and Hach DR6000 UV-VIS spectrophotometer with 1 cm quartz cuvette (Loveland, CO, USA) were used, respectively. COD and volatile fatty acid (VFA) tests were conducted using Hach colorimetric methods (Loveland, CO, USA). Standard methods were followed for BOD_5, TS, and TSS measurement (APHA, 2012). Raw leachate characteristics are as listed in Table 1.

Raw landfill leachates were further characterized using elemental analysis. For elemental analysis, samples were first freeze dried using Labconco lyophilizer under −50 °C and 0.03 Mbar pressure and then shipped to Elemental Analysis, Inc lab (Kentucky, USA) for elemental analysis. PerkinElmer 2400 (Waltham, MA, USA) was used for C, H, and N analysis.

UV–vis analysis was also applied to organic fractions isolated from raw landfill leachates. The UV–Vis spectra were recorded on a Hach DR6000 UV Vis spectrophotometer (Loveland, CO, USA) using a 1 cm quartz cell. The spectra of the samples were obtained over a wavelength range of 300–800 nm and absorbance at 254 and 280 nm were also measured. Specific ultraviolet absorbance at 254 nm ($SUVA_{254}$) was also calculated as UV_{254} absorbance divided by DOC.

For FTIR analysis, raw leachate samples in a freeze-dried form were used. The samples for FTIR spectra were obtained by mixing the solid samples with an infrared-inactive material KCl (200 mg KCl + 2.5 mg freeze dried sample). Pellets were prepared by applying hydraulic pressure on the mixtures. Resulting pellets were then analyzed on a Nicolet IS50 FT-IR spectrophotometer (Thermo Fisher Scientific,

Table 1
Raw leachate properties.

Parameters	Site-A		Site-B	
	Non-impacted	Impacted	Non-impacted	Impacted
pH	8.04	5.74	8.57	5.4
BOD_5 (mg L^{-1})	1314	34764	3731	39379
COD (mg L^{-1})	8230	81200	16925	93800
BOD_5/COD	0.16	0.43	0.22	0.42
TOC	2638	27319	4988	32935
VFA (mg L^{-1}) as CH_3COOH	785	22850	1628	27700
UV_{254} absorbance (cm^{-1})	0.44	2.64	1.28	2.35
$SUVA_{254}$ (L mg^{-1} m^{-1})	1.67	0.97	2.57	0.71
UV_{280} absorbance (e_{280}, cm^{-1})	3.27	2.58	3.04	1.64

Waltham, MA, USA) in the range of 4000–400 cm^{-1} with average scans of 64 and spectral resolution of 4 cm^{-1}.

2.3. Organic matter fractionation

For leachate organic matter fractionation, a method from previous studies (Valencia et al., 2013; Zhao et al., 2013; Iskander et al., 2018) was used. More details of the leachate organic matter fractionation method can be found in Supporting Information, section S1.

2.4. Negative-ion electrospray ionization Fourier-transform ion cyclotron resonance mass spectrometry (FT-ICR MS) analysis

To identify compositional changes between dissolved organic species in impacted leachates, dissolved compounds were extracted by solid phase microextraction on styrene-divinylbenzene (SDVB) polymer modified with a proprietary nonpolar surface (Bond Elute Priority Pollutant™, Agilent Technologies) prior to ESI 21 T FT-ICR MS (Hendrickson et al., 2015) based on Dittmar et al. Briefly, samples were diluted in 100% HPLC-grade methanol (J.T. Baker Chemical Company) and analyzed in negative-ion electrospray ionization mode (-ESI) with a custom-built hybrid linear ion trap FT-ICR mass spectrometer equipped with a 21 T superconducting solenoid magnet (Hendrickson et al., 2015) at the National High Magnetic Field Laboratory in Tallahassee, Florida.

Complete experimental details of the FT-ICR MS analysis can be found in Supporting Information, section S2. All FT-ICR MS data files and elemental compositions are publicly-available via the Open Science Framework at https://osf.io/y6chk/.

3. Results & discussion

3.1. Aggregate organics of leachate

For both landfill sites, impacted leachates had higher organic content than non-impacted leachates in terms of BOD_5, COD, and TOC (Table 1). The BOD_5/COD ratio was higher in impacted leachates from both sites. Since BOD_5 is more labile than COD, the ratio of BOD_5 to COD varies from 0.5 for a relatively 'fresh' leachate to 0.2 for relatively stabilized leachate (Tatsi and Zouboulis, 2002). Additionally, the pH of impacted leachate was found to be more acidic than non-impacted leachate for landfill sites.

The VFA analysis showed that impacted leachate from landfill sites had significantly higher concentration of VFAs than non-impacted leachate. Factoring the VFA concentration, organic matter, and pH values of the impacted leachate from both sites seems to indicate towards a biochemical cause during the decomposition of the waste. Based on the previous studies it can be said that the methanogenic activities are interfered in the high temperature zones, with conversion of VFAs to methane gas also gets impeded (Hartz et al., 1982; Jafari et al., 2017a, 2017b; Martin et al., 2013; Schupp et al., 2021; Stark et al., 2012), which partially explains the higher organic content in impacted leachates. Methanogenic bacteria degrade the VFAs and reduce the organic strength of leachate, leading to a pH higher than 7.0 during the methanogenic phase, hence, the non-impacted leachates can be considered to have been undergone methanogenic phase (Kurniawan et al., 2006). In ETLFs, methanogens are inhibited by the high-temperature and VFAs are accumulated consequently, causing acidic conditions. Also, the higher solids content in impacted leachates is partially attributed to the acidic pH that mobilizes cations, such as iron. Hence, the impacted leachates from both sites were acidic, whereas non-impacted leachates were alkaline. Higher VFAs in impacted leachates implied that the degree of aromaticity was lower in the impacted leachates as VFAs are short-chain aliphatic carboxylate compounds.

3.2. UV spectra of leachate

The overall UV_{254} absorbance of the non-impacted leachates was less than the impacted leachates (Table 1). However, the specific UV_{254} absorbance ($SUVA_{254}$) or the UV_{254} absorbance by unit organic carbon of the non-impacted leachates was greater than impacted ones. Following the $SUVA_{254}$ trend, non-impacted leachates had higher absorbance at 280 nm (e_{280}) than impacted leachates. Higher $SUVA_{254}$ and e_{280} values in non-impacted leachates indicated that non-impacted leachates had greater degree of aromaticity than the impacted leachates. The degree of aromaticity of the leachate samples can further be confirmed by the FTIR analysis of the same leachate samples reported by Patel et al. (2021) (see Fig. 7 of the cited work).

Overall, between non-impacted and impacted leachates, impacted leachates had higher organic content with a higher percentage of the biodegradable fraction compared to the non-impacted leachates. Impacted leachates had higher VFA content (aliphatic short-chain carboxylates) and H/C ratio, while $SUVA_{254}$ and e_{280} values were lower in impacted leachates. This indicates that the degree of aromaticity was lower in the impacted leachates than in non-impacted leachates.

3.3. Elemental composition of leachate

As shown in Table 2, the results of elemental analysis for leachate samples were normalized to 100 wt% of organic components for right comparison. The results of elemental analysis (Table 2) for leachate samples further confirmed the lower degree of aromaticity in the impacted leachates.

Percentage of C and H were higher in impacted leachates than that in non-impacted leachates and percentage of O was higher in non-impacted leachates than that in impacted leachates for both the sites. Precise interpretation can be done by looking at the atomic ratios of H/C and O/C from the elemental composition for the leachates. H/C ratio clustered around 1.0 implies a chemical structure consisting predominantly of aromatic framework (Steelink, 1985; Kang et al., 2002). Non-impacted leachates of site-A and site-B had H/C ratio of 1.68 and 1.84, respectively and impacted leachates of site-A and site-B had H/C ratio of 2.09 and 2.18, respectively. Thus, the high H/C ratio in impacted leachates implied that they contained significant portions of aliphatic functional groups and low H/C ratio in non-impacted leachates implied that they contained more aromatic structure framework. Also, a higher O/C ratio of non-impacted leachates than impacted leachates indicated a high content of oxygen containing carbohydrates in non-impacted leachates (Kang et al., 2002).

3.4. Organic fractions in landfill leachates

Concentration of the organic fractions in the untreated samples were measured as TOC and COD. In the non-impacted leachates, HA concentrations were 689 mg $L^{-1}$and 1,549 mg L^{-1}in terms of TOC in site-A and site-B, respectively, while FA concentrations were 754 mg L^{-1} and 1,364 mg L^{-1} in the two sites, respectively (Fig. 1a). The total HS

Table 2
Elemental composition and ratios of leachates.

Elemental composition and ratios	Site-A		Site-B	
	Non-impacted	Impacted	Non-impacted	Impacted
C (w/w%)[a]	37.15	41.59	37.53	40.89
H (w/w%)[a]	5.20	7.25	5.78	7.42
N (w/w%)[a]	3.65	5.26	3.99	3.50
O (w/w%)[a]	54.00	45.90	52.7	48.19
H/C[b]	1.68	2.09	1.84	2.18
O/C[b]	1.09	0.82	1.05	0.88

[a] Elemental composition normalized to 100 wt% of organic components.
[b] Molar ratio.

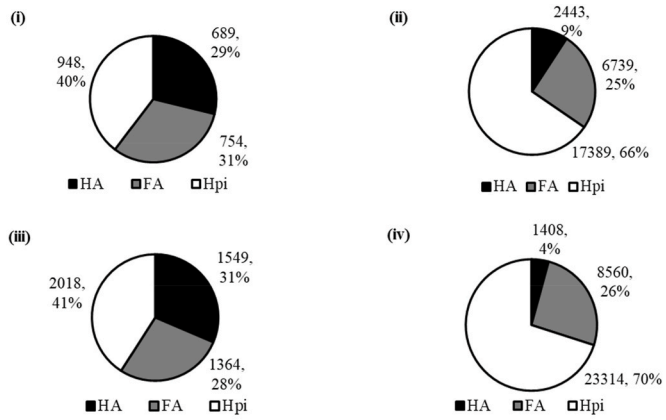

(a) Values (mg L^{-1}) and distribution (%) of humic substance fractions as TOC.

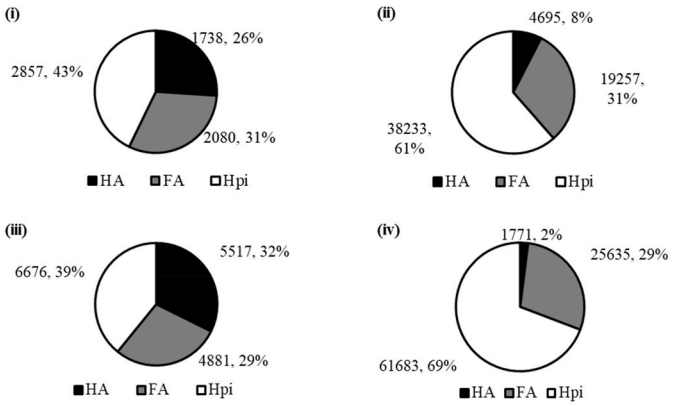

(b) Values (mg L^{-1}) and distribution (%) of humic substance fractions as COD

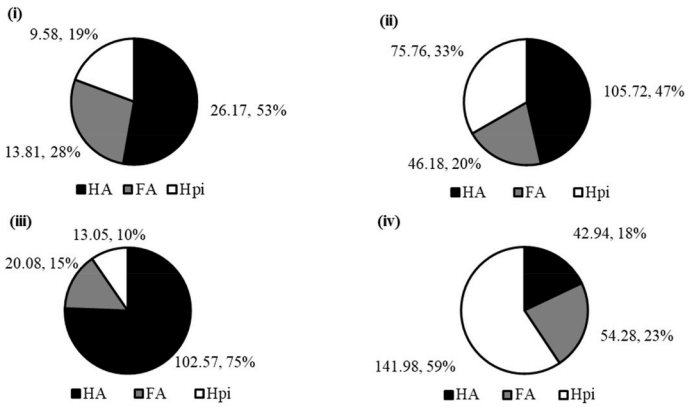

(c) Values (m^{-1}) and distribution (%) of humic substance fractions as UV_{254} absorbance.

Fig. 1. Values and distribution of isolated HS fractions in terms (a) TOC, (b) COD, and (c) UV_{254} absorbance in (i) non-impacted and (ii) impacted leachates from site-A, and (iii) non-impacted and (iv) impacted leachates from site-B.

concentration therefore was 1,443 mg L^{-1} and 2,913 mg L^{-1} in site-A and site-B, respectively. The total HS content constituted 60% and 59% of the total TOC in the non-impacted leachates, respectively. In contrast, the impacted leachates in site-A and site-B had 2,443 mg L^{-1} and 1,408 mg L^{-1} of HA, and 6,739 mg L^{-1} and 8,560 mg L^{-1} of FA, respectively. The total HS content in impacted leachates were 9,182 mg L^{-1} and 9,968 mg L^{-1} which constituted 35% and 30% of total TOC in the impacted leachates in site-A and site-B, respectively. Therefore, comparing the HS distribution, both non-impacted and impacted leachates had same percentage of FA while HA percentage was higher in non-impacted leachates than in impacted leachates. Hence, the total percentage of HS fractions were higher in non-impacted leachates than in impacted leachates. Concentration and distribution of HS fractions in terms of COD followed the same trend as in TOC concentration and distribution (Fig. 1b). As stated earlier, the impacted leachates were acidic, meaning methanogenesis was interrupted and the high temperature in the impacted zones resulted in accumulation of VFAs. Notably, non-impacted leachates in site-A and site-B had 785 and 1,628 mg L^{-1} VFA as CH_3COOH while impacted leachates had higher VFAs, 22,850 and 27,700 mg L^{-1} as CH_3COOH in site A and site B, respectively (Table 1). In non-impacted zones, VFAs were degraded with methanogen. Hence, non-impacted leachates had overall higher percentage of HS than impacted leachates.

In the non-impacted leachates, UV_{254} absorbance was in the order of HA > FA > Hpi. The HA fraction absorbed 26 m^{-1} and 103 m^{-1} while FA absorbed 14 m^{-1} and 20 m^{-1} UV_{254} in site-A and site-B, respectively (Fig. 1c). The Hpi fraction of the non-impacted leachates from site-A and site-B absorbed 10 m^{-1} and 13 m^{-1} UV_{254}, respectively. The distribution of the UV_{254} absorbance among the HS fraction in the non-impacted leachates showed that the cumulative UV_{254} absorbance caused by HA and FA accounts for 81% and 90% of the total UV_{254} absorbance (Fig. 1c). In the impacted leachates, UV_{254} absorbance by HA fraction was 106 m^{-1} and 43 m^{-1} while UV_{254} absorbance by FA fraction was 46 m^{-1} and 54 m^{-1} in site-A and site-B, respectively. The Hpi fraction absorbance in the impacted leachates was 76 m^{-1} and 142 m^{-1} respectively in site-A and site-B. The distribution of UV_{254} absorbance among the HS fractions in impacted leachate showed the cumulative absorbance by HA and FA accounted for 67 % and 41% total UV_{254} absorbance. It was observed that UV_{254} absorbance by FA was lower than Hpi fractions in the impacted leachates. Generally, HS fractions absorb UV_{254} greater than the Hpi fractions because of greater degree of aromaticity in HS. The reason for FAs absorbing lower UV_{254} than Hpi in impacted leachate could be that the concentration of Hpi fractions is relatively higher in the impacted leachates (see Fig. 2a for concentration of the HS fractions).

3.5. Leachate humic substance aromaticity

The amount of UV_{254} absorbance can better be understood by analyzing the $SUVA_{254}$ and e_{280} values of the isolated fractions as it can be regarded as a tool to characterize the degree of humification and aromaticity of organic matter (Cheng et al., 2005; Wang et al., 2016). The $SUVA_{254}$ of HA was always greater in all the leachates (Fig. 2a). Although the percentage of UV_{254} absorbed by HA and FA was lower than the absorbance by Hpi in the impacted leachate from site-B, $SUVA_{254}$ of HA and FA was still greater than that of Hpi. Lower percentage of UV_{254} absorbance by humic acid in the impacted leachate from site-B was due to the very low percentage of humic acid present in it (Fig. 1c). Overall, $SUVA_{254}$ and e_{280} values were in the order of HA > FA > Hpi for all the leachates (Fig. 2a and b). Higher $SUVA_{254}$ and e_{280}

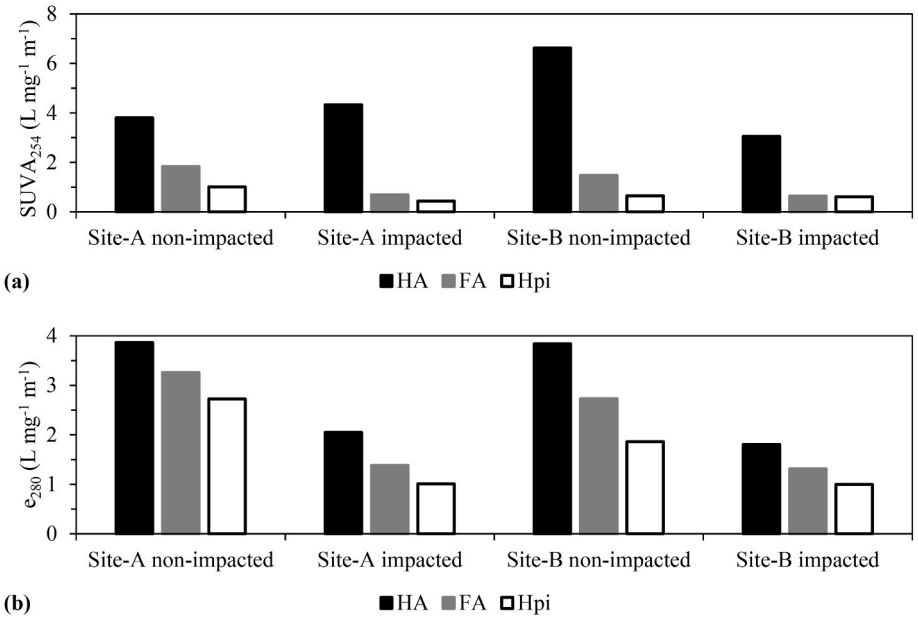

Fig. 2. (a) $SUVA_{254}$ and (b) e_{280} values of the isolation humic substances in leachates before treatment.

in HA was due to having greater degree of aromaticity and high molecular weight as studies showed that aromaticity and molecular weight are positively correlated to higher specific absorbance, $SUVA_{254}$ and e_{280}, in this case (Chin and Aiken, 1994; Gaffney et al., 1996; Weishaar et al., 2003).

The degree of aromaticity and characteristics of the isolated HS fractions were further analyzed using FTIR (Fig. 3). HA and FA fractions of non-impacted leachates showed absorption bands at 3400 cm^{-1} due to intermolecular OH stretching, 2930 cm^{-1} due to aliphatic CH stretching, 1690 cm^{-1} - 1710 cm^{-1} and 1240 cm^{-1} due to C═O stretching of –COOH and ketonic C═O, 1500 cm^{-1} - 1510 cm^{-1} due to N–O stretching and 1440 cm^{-1} due to CH methyl and methylene groups of aliphatic compounds. However, at 1630 cm^{-1}, HA fraction showed a sharp peak whereas FA showed an inconspicuous signal which is a characteristic distinction between HA and FA (Li et al., 2014). The peak at 1630 cm^{-1} is due to the stretching of C═C benzene rings. This peak indicated that HA had more aromatic carbons than FA, which agrees with the $SUVA_{254}$ and e_{280} data from UV–Vis spectroscopy. HA showed little more absorption at 1580 cm^{-1}– 1650 cm^{-1} due to the stretching of C–N amides (Qi et al., 2012).

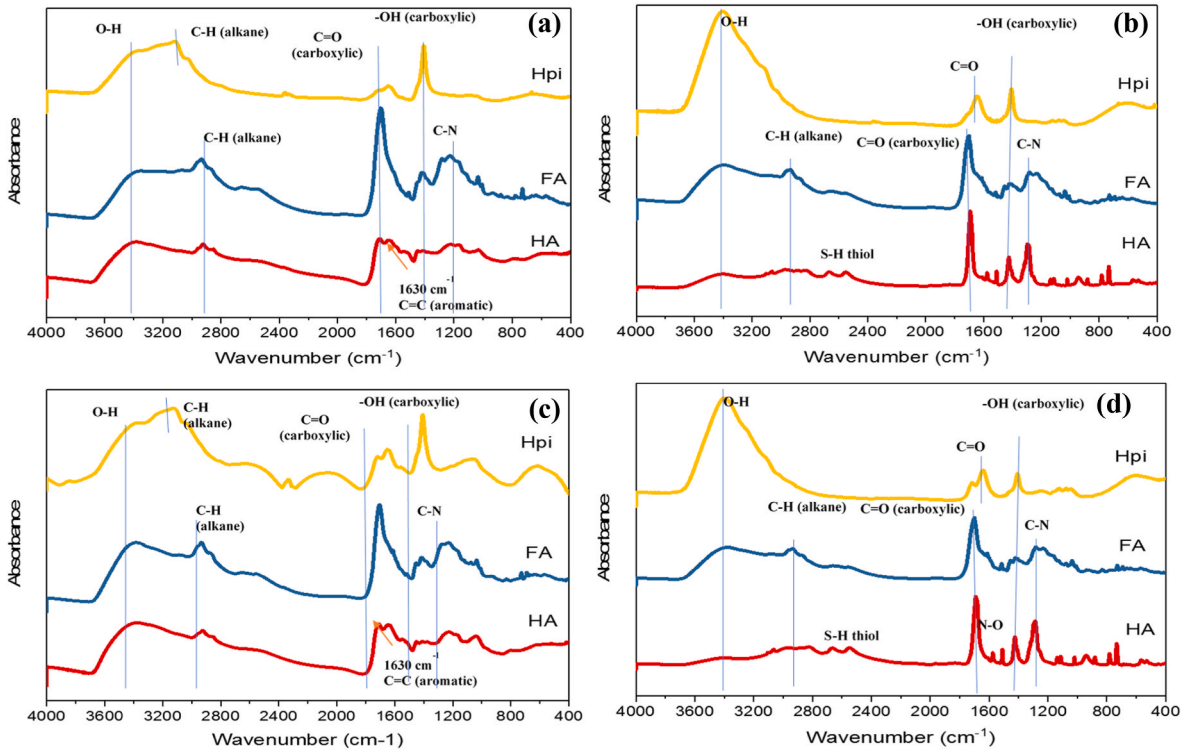

Fig. 3. Fourier-transform IR spectra of isolated humic substances of (a) non-impacted, (b) impacted leachate from site-A, and (c) non-impacted, (d) impacted leachate from site-B.

FA, on the other hand, had more absorption as compared to HA in the range 1690 cm^{-1} - 1710 cm^{-1} and 1200 cm^{-1} – 1230 cm^{-1}, which is due to C═O stretching of –COOH and OH bending of carboxylic acids, respectively, as mentioned earlier. The FA fraction, thus may be more acidic than HA (Kang et al., 2002). Also, more absorption at 1720 cm^{-1} by FA indicated a greater amount of oxygen-containing groups in FA (Chai et al., 2007). The FA and Hpi fractions showed higher absorption for aliphatic compounds (3333 cm^{-1} – 2840 cm^{-1}) than HA. This finding coincided with literature (Christensen et al., 1996) on landfill leachate polluted groundwater. Also, as compared to HA, Hpi had a dominating peak at 1400 cm^{-1}, which is due to O–H bending of carboxylic acid. Thus, the FTIR spectra of the HS fractions of non-impacted leachates indicated HA has greater degree of aromaticity than FA and Hpi.

For impacted leachate HS fractions, the spectra of impacted leachates - FA and Hpi resembled the spectra of non-impacted leachates - FA and Hpi implying the presence of the same functional groups in them.

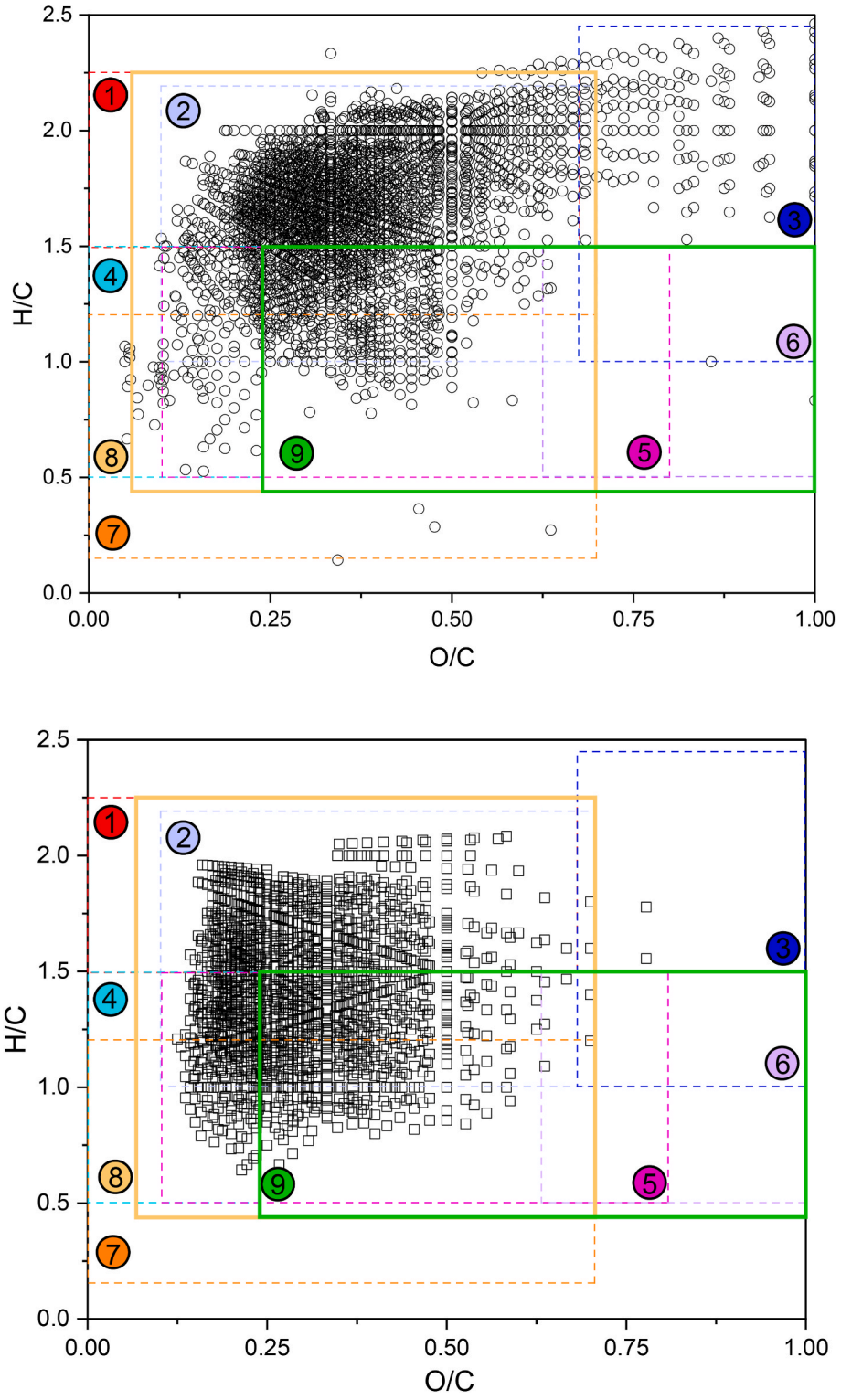

Fig. 4. Van Krevelen diagram for elemental composition of leachate B non-impacted (top) and leachate B impacted (bottom).

However, impacted leachate HA showed more complex absorption bands than non-impacted leachates. The common absorption bands were: 3400 cm^{-1} due to intermolecular OH stretching, 2930 cm^{-1} due to aliphatic CH stretching, 1620 cm^{-1} -1610 cm^{-1} by aromaticity, and 1510 cm^{-1} - 1500 cm^{-1} due to N–O stretching. Impacted leachates HA showed significant peaks between 2600 cm^{-1} -2550 $cm^{-1,}$ which is attributed by S–H thiol group, 1300 cm^{-1} due to stretching of S═O sulphone group, 1425 cm^{-1} due to bending of O–H of alcohol and it also showed more complicated absorption bands at low wavenumbers due to halogenated compounds. In other words, HA of impacted leachates was like HA of non-impacted leachates except that HA of impacted leachates showed more sulfur-containing functional groups, alcoholic compounds, and halo-compounds. Overall, the HA and FA fraction in the impacted leachates also showed greater degree of aromaticity as evidenced by the spectral analysis: $SUVA_{254}$, e_{280}, and FTIR. For all leachate samples, the degree of aromaticity among the HS fractions was in the order of HA > FA > Hpi.

3.6. Fourier-transform ion cyclotron resonance mass spectrometry (FTICR-MS)

Fig. 4 shows the H:C versus O:C ratios for detected elemental composition above 0.25% relative abundance in leachate B non-impacted (top) and leachate B impacted (bottom). The 9 regions shown in Fig. 4 indicate the 9 different organic matter groups listed in Table 3. Among the typical hydrocarbons found in leachate, leachate B non-impacted had lipids, proteins and amino acids, lignin, unsaturated hydrocarbons, condensed aromatics, and carbohydrates. The abundance of these hydrocarbons was in the order of lipids > proteins and amino acids > lignin > unsaturated hydrocarbons > condensed aromatics > carbohydrates. Tannin was found to be the least abundant among all groups. The majority of elemental compositions had O: C between 0.1 and 0.6 and H:C between 0.5 and 2.2. For leachate B impacted, the organic group found were lipids, proteins and amino acids, unsaturated hydrocarbons, lignin, and condensed aromatics. The relative abundance of the elemental composition in impacted leachate B was in the order of unsaturated hydrocarbons > lignin > lipids > proteins and amino acids > condensed aromatics. For impacted leachate, the majority of the compounds were found with H:C between 1 and 1.75 and O:C between 0.1 and 0.5.

One of the main differences between non-impacted and impacted leachate was the presence of carbohydrates. The non-impacted leachate had significant carbohydrates present, while the impacted leachate had almost none. The difference in presence of carbohydrates is possibly due to the hydrolysis and acidogenesis processes that were enhanced by the elevated temperature. Acidogenic bacteria are able to survive at high temperatures (Yuan et al., 2019). Generally, hyperthermophilic (>65 °C) conditions improve the hydrolysis and acidogenesis processes compared to mesophilic conditions (25–45 °C) (Fang et al., 2020; Lee et al., 2014; Yuan et al., 2019). The carbohydrates in the impacted leachate were possibly completely consumed by the elevated temperature enhanced acidogenesis process, while residual carbohydrates remain in the non-impacted leachate as hydrolysis and acidogenesis were not complete.

Table 3
FT-ICR MS elemental ratio values for various chemical compound groups determined from elemental compositions derived from negative-ion ESI FT-ICR MS (Sleighter and Hatcher, 2007; Hertkorn et al., 2008; Hockaday et al., 2009; Ohno et al., 2010; Yuan et al., 2017; Rivas-Ubach et al., 2018; Goranov et al., 2022; Ikeya et al., 2012; Visser, 1983).

No.	Chemical compound groups	H:C	O:C
1	Lipids	1.5–2.25	0.0–0.7
2	Proteins and amino acids	1.0–2.2	0.1–0.83
3	Carbohydrates	1.0–2.4	0.67–1.3
4	Unsaturated Hydrocarbons	0.5–1.5	0.0–0.23
5	Lignin	0.5–1.5	0.1–0.8
6	Tannin	0.5–1.5	0.63–1.0
7	Condensed Aromatics	0.2–1.2	0.0–0.7
8	Humic Acids	0.4–2.25	0.1–0.7
9	Fulvic Acids	0.4–1.5	0.25–1.0

Lipids were found to be present in both non-impacted and impacted leachate. However, lipids can be found as saturated (H:C = 1.8–2 and O:C = 0–0.15) and unsaturated (H:C = 1.4–1.8 and O:C = 0–0.15) (Jiménez-González et al., 2020). Comparing above information and the elemental ratio data shown in the lipid region in Fig. 4, it suggests that non-impacted leachate contains more saturated lipids, while impacted leachate contains more unsaturated lipids. For both non-impacted and impacted leachate, tannin (H:C = 0.5 to 1.5 and O:C = 0.63 to 1.0) was found to be the least abundant organic group among all.

Furthermore, a cluster data points of elemental ratio can be found for both non-impacted leachate and impacted leachate in Fig. 4. For non-impacted leachate, a higher signal density was found in the region H:C > 1.5 and O:C = 0.1 to 0.75, while for impacted leachate, a higher signal density is seen in the region H:C < 1.5 and O:C = 0.1 to 0.5. This indicates that non-impacted leachate contains more lipids, proteins-amino acids, and carbohydrates, while impacted leachate contains more unsaturated hydrocarbon and lignin.

In terms of the presence of humic acids in both the leachate samples, Fig. 4 (top) shows that non-impacted leachate had much higher volume of humic acids compared to impacted leachate which is supported by TOC and COD distribution in Fig. 1a and (b). Based on the overlapping of elemental ratios of humic acids (region 8) with all other chemical compound groups, it can be seen that majority of the humic acids is derived from lignin (region 5), unsaturated hydrocarbons (region 4), and condensed aromatics (region 7) that may have gone through humification. Humic acids derived from lignin were higher in non-impacted leachate (Fig. 4 top) than in impacted leachate (Fig. 4 bottom). In impacted leachate (Fig. 4 bottom), more humic acids seem to have been derived from unsaturated carbon (region 4) and condensed aromatic compounds (region 7). The trend of fulvic acids in both non-impacted and impacted leachate samples is found to be similar, which was also observed from TOC and COD distribution in Fig. 1(a) and (b). Fulvic acids (region 9) in both non-impacted and impacted leachate samples were found possibly be derived from lignin (region 5) and condensed aromatic compounds (region 7) based on signal overlapping. Based on Fig. 4 (top and bottom), extremely low sources of fulvic substances were found from tannin (region 6) compared to other sources.

Fig. 5 shows H/C versus O/C of elemental species for both non-impacted and impacted leachate based on aromaticity. Because FT-ICR MS characterization of complex organic mixtures such as leachate results in the identification of tens of thousands of individual species, Van Krevelen diagrams provide a visual tool to rapidly compare the compositional differences between samples. Van Krevelen diagrams plot the atomic H/C versus O/C ratio to approximate oxidation state, compositional information to biological precursors, and hydrogen deficiency (e.g., DBE, double bond equivalent, number of rings plus double bonds to carbon, DBE = C -h/2 + n/2 + 1, or aromaticity index, AI) to approximate bioavailability. Molecular formulae can be grouped in compound classes based on H/C and O/C ranges, with regions of the van Krevelen diagram tentatively associated with certain compound classes (e.g., lipids O/C < 0.2, H/C 2.0+), or condensed hydrocarbons (O/C < 0.2, H/C < 1), in addition to cellulose-like, lignin-like, peptide-like and sugar-like regions.

The aromatic index was calculated for detected neutral species using the formula given below.

$$Aromaticity\ Index = \frac{1 + C - O - S - 0.5H}{C - O - S - N - P}$$ (Koch and Dittmar, 2006)

Each point corresponds to an elemental composition, colored by A.I.: non-aromatic (hollow, A.I. ≤ 0.5), aromatic (grey, 0.67 > A.I. > 0.5), and condensed aromatic (solid, A.I. ≥ 0.67). Species detected in non-

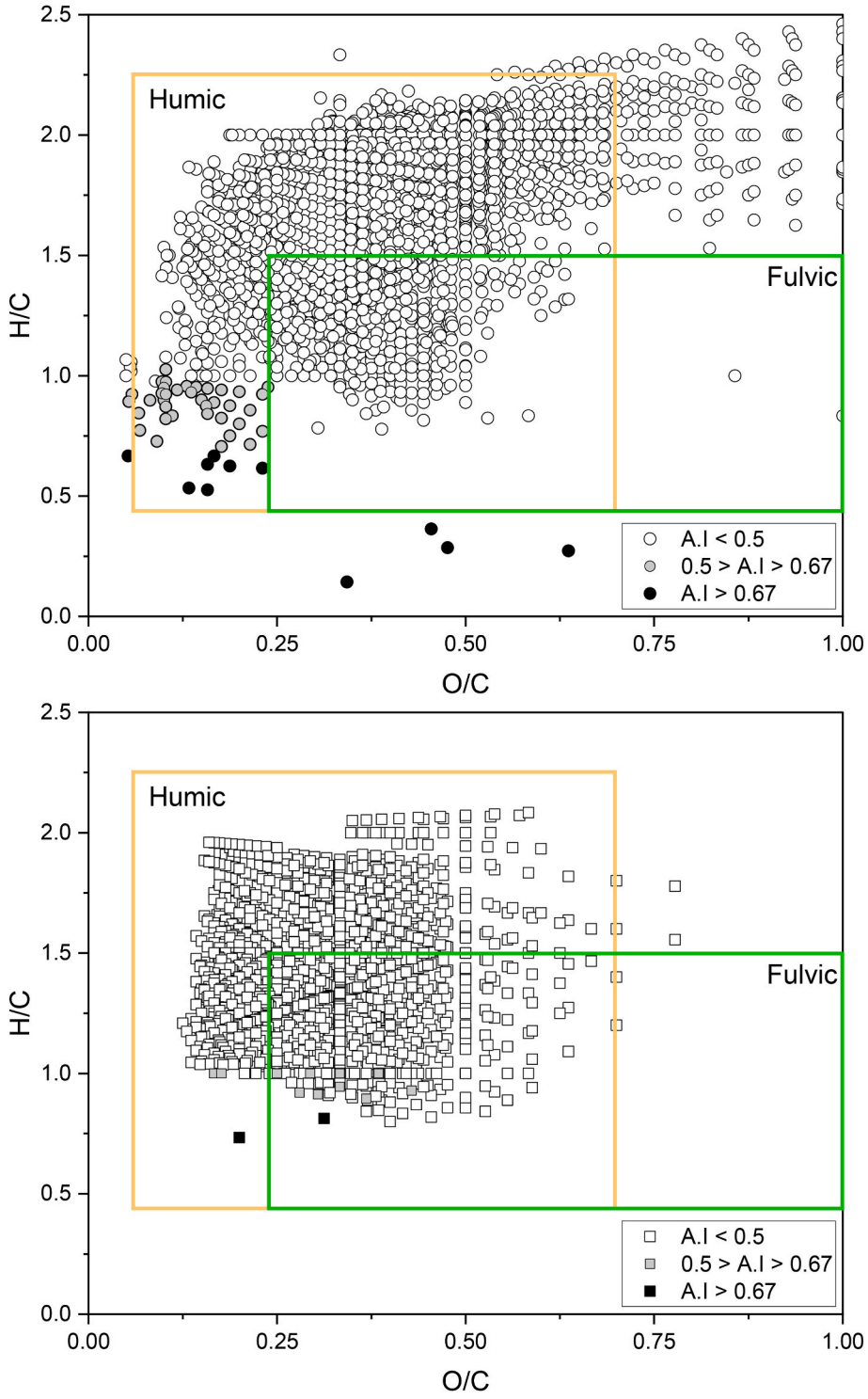

Fig. 5. Van Krevelen diagram for elemental composition of leachate B non-impacted (top) and impacted leachate (bottom) based on aromaticity.

impacted leachate correspond to H/C ratios between 0.5 and 2.5, whereas species in impacted leachate range from 0.75 to 2.1. In addition, acidic species detected in impacted leachate have much lower O/C ratios (0.1–0.7) compared to non-impacted, which had a higher O/C ratio for detected species (0.18–1.0). Based on Fig. 5, results clearly indicate that more aromatic compounds were detected in non-impacted leachate than in impacted leachate. Hence, it supports the experimental results from organic fractionation of leachate, that non-impacted leachate has more aromaticity than impacted leachate. It can also be observed that in non-impacted leachate, more aromatic and condensed aromatic species are present in the humic acid region, but for impacted leachate aromatic and condensed aromatics are found in the fulvic acid region.

4. Conclusions

Comparison of characteristics of leachates from impacted and non-impacted zones in ETLFs indicated inhibition of methanogenesis and enhancement of hydrolysis and acidogenesis by the elevated temperature. High level of VFA was found in leachates from temperature-

impacted zones of both landfill sites, which was evidence that the conversion of VFA to methane gas was interfered with by the elevated temperature (80–100 °C). More acidic pH (5.4–5.7), higher BOD (34,000–40,000 mg L^{-1}), and BOD/COD ratio (0.42–0.43) further confirmed the existence of higher VFA in impacted leachates. In addition, impacted leachate showed lower aromatic properties based on lower SUVA (0.71–0.97), and H/C ratio (2.09–2.18), as most VFAs are short-chain aliphatic hydrocarbons. Depletion of carbohydrates in an elevated temperature impacted landfill leachate was observed by comparing the FTICR spectra of impacted and non-impacted leachate samples from the same landfill, which indicated possible enhancement of hydrolysis and acidogenesis processes by the elevated temperature.

The distribution of HS fractions showed a pattern of lower percentage of total HS fractions in leachates from impacted zones by elevated temperature, ostensibly due to accumulation of VFA as methanogenic activities were likely inhibited by the elevated temperature in the zones. The $SUVA_{254}$ and e_{280} values for the isolated HS fractions were in the order of HA > FA > Hpi, indicating HA should be agreed with the most UV_{254} absorbing as HA typically has greater degree of aromaticity and is of higher molecular weight causing greater potential for UV_{254} absorbance. The FTIR analysis of the isolated HS fractions further confirmed greater degree of aromaticity in the HA fractions of the leachate samples. FTICR-MS results for leachate B non-impacted and impacted also support that non-impacted have higher concentration of humic substances and degree of aromaticity than impacted leachate.

This study sheds light on the path using leachate characteristics to indicate the chemical and biochemical activities in landfills.

Credit author statement

Synthia P. Mallick: Investigation, Methodology, Writing – original draft, Visualization, Harsh V. Patel: Investigation, Formal analysis, Writing – original draft. Sailee Gawande: Investigation, Alfred Wadee: Investigation, Huan Chen: Resources, Formal analysis, Amy M. McKenna: Resources, Formal analysis, Brian Brazil: Resources, Funding acquisition, Wenzheng Yu: Validation, Writing – review & editing, Renzun Zhao: Conceptualization, Resources, Writing – review & editing, Supervision, Project administration, Funding acquisition.

Declaration of competing interest

The authors declare that they have no known competing financial interests or personal relationships that could have appeared to influence the work reported in this paper.

Data availability

Data will be made available on request.

Acknowledgement

This work was supported by National Science Foundation (CBET 2101053) and Waste Management Inc. Synthia P Mallick (S.P.M.) earnestly thanks American Association of University of Women (AAUW) for supporting her through the International Fellowship. The Ion Cyclotron Resonance user facility is funded by the National Science Foundation Division of Materials Research and Division of Chemistry through (DMR-2128556), and the State of Florida. Harsh V. Patel (H.V.P.) earnestly thanks HDR Inc. for supporting him through the HDR Water Scholarship.

Appendix A. Supplementary data

Supplementary data to this article can be found online at https://doi.org/10.1016/j.jenvman.2023.119719.

References

Adhikari, B., Dahal, K.R., Khanal, S.N., 2014. A review of factors affecting the composition of municipal solid waste landfill leachate. International journal of engineering science and innovative technology 3 (5), 273–281.

Bahureksa, W., Borch, T., Young, R.B., Weisbrod, C.R., Blakney, G.T., McKenna, A.M., 2022. Improved dynamic range, resolving power, and sensitivity achievable with FT-ICR mass spectrometry at 21 T reveals the hidden complexity of natural organic matter. Anal. Chem. 94 (32), 11382–11389. https://doi.org/10.1021/acs.analchem.2c02377.

Chai, X., Takayuki, S., Cao, X., Guo, Q., Zhao, Y., 2007. Spectroscopic studies of the progress of humification processes in humic substances extracted from refuse in a landfill. Chemosphere 69, 1446–1453. https://doi.org/10.1016/j.chemosphere.2007.04.076.

Cheng, W., Dastgheib, S.A., Karanfil, T., 2005. Adsorption of dissolved natural organic matter by modified activated carbons. Water Res. 39, 2281–2290. https://doi.org/10.1016/j.watres.2005.01.031.

Chin, Y.-Pi, Aiken, G., 1994. Molecular weight, polydispersity, and spectroscopic properties of aquatic humic substances. Environ. Sci. Technol. https://doi.org/10.1021/es00060a015.

Christensen, J.B., Jensen, D.L., Christensen, T.H., 1996. Effect of dissolved organic carbon on the mobility of cadmium, nickel and zinc in leachate polluted groundwater. Water Res. 30, 3037–3049. https://doi.org/10.1016/S0043-1354(96)00091-7.

Cossu, R., Polcaro, A.M., Lavagnolo, M.C., Mascia, M., Palmas, S., Renoldi, F., 1998. Electrochemical treatment of landfill leachate: oxidation at Ti/PbO2 and Ti/SnO2 anodes. Environ. Sci. Technol. 32, 3570–3573. https://doi.org/10.1021/es971094o.

De la Cruz, F.B., Cheng, Q., Call, D.F., Barlaz, M.A., 2021. Evidence of thermophilic waste decomposition at a landfill exhibiting elevated temperature regions. Waste Manag. 124, 26–35. https://doi.org/10.1016/j.wasman.2021.01.014.

Deng, Y., Englehardt, J.D., 2006. Treatment of Landfill Leachate by the Fenton Process. Water Research. https://doi.org/10.1016/j.watres.2006.08.009.

Dittmar, T., Koch, B., Hertkorn, N., Kattner, G., 2008. A simple and efficient method for the solid-phase extraction of dissolved organic matter (SPE-DOM) from seawater. Limnol Oceanogr. Methods 6 (6), 230–235. https://doi.org/10.4319/lom.2008.6.230.

Dubnick, Ashley, Faber, Q., Hawkings, J.R., Bramall, N., Christner, B.C., Doran, Peter T., Nadeau, Jay, et al., 2022. Biogeochemical responses to mixing of glacial meltwater and hot spring discharge in the Mount St. Helens crater. J. Geophys. Res.: Biogeosciences 127 (10), e2022JG006852. https://doi.org/10.1029/2022JG006852.

Ehrig, H.-J., 1989. Water and element balances of landfills. In: Baccini, P. (Ed.), The Landfill, Lecture Notes in Earth Sciences. Springer, Berlin, Heidelberg, pp. 83–115. https://doi.org/10.1007/BFb0011259.

El-Fadel, M., Findikakis, A.N., Leckie, J.O., 1997. Environmental impacts of solid waste landfilling. J. Environ. Manag. 50, 1–25. https://doi.org/10.1006/jema.1995.0131.

Fang, W., Zhang, X., Zhang, P., Wan, J., Guo, H., Ghasimi, D.S., Morera, X.C., Zhang, T., 2020. Overview of key operation factors and strategies for improving fermentative volatile fatty acid production and product regulation from sewage sludge. J. Environ. Sci. 87, 93–111. https://doi.org/10.1016/j.jes.2019.05.027.

Gaffney, J.S., Marley, N.A., Clark, S.B., 1996. Humic and fulvic acids and organic colloidal materials in the environment. ACS (Am. Chem. Soc.) Symp. Ser. 651 https://doi.org/10.1021/bk-1996-0651.ch001.

Goranov, A.I., Tadini, A.M., Martin-Neto, L., Bernardi, A.C.C., Oliveira, P.P.A., Pezzopane, J.R.M., Milori, D.M.B.P., Mounier, S., Hatcher, P.G., 2022. Comparison of sample preparation techniques for the (−)ESI-FT-ICR-MS analysis of humic and fulvic acids. Environ. Sci. Technol. 56, 12688–12701. https://doi.org/10.1021/acs.est.2c01125.

Hanson, J.L., Yeşiller, N., Onnen, M.T., Liu, W.L., Oettle, N.K., Marinos, J.A., 2013. Development of numerical model for predicting heat generation and temperatures in MSW landfills. Waste Manag. 33, 1993–2000. https://doi.org/10.1016/j.wasman.2013.04.003.

Hao, Z., Sun, M., Ducoste, J.J., Benson, C.H., Luettich, S., Castaldi, M.J., Barlaz, M.A., 2017. Heat generation and accumulation in municipal solid waste landfills. Environ. Sci. Technol. 51, 12434–12442. https://doi.org/10.1021/acs.est.7b01844.

Hartz, K.E., Klink, R.E., Ham, R.K., 1982. Temperature effects: methane generation from landfill samples. J. Environ. Eng. Div. 108, 629–638. https://doi.org/10.1061/JEEGAV.0001314.

Hendrickson, C.L., Quinn, J.P., Kaiser, N.K., Smith, D.F., Blakney, G.T., Chen, T., Marshall, A.G., Weisbrod, C.R., Beu, S.C., 2015. 21 Tesla Fourier transform ion cyclotron resonance mass spectrometer: a national resource for ultrahigh resolution mass analysis. J. Am. Soc. Mass Spectrom. 26 (9), 1626–1632. https://doi.org/10.1007/s13361-015-1182-2.

Hertkorn, N., Frommberger, M., Witt, M., Koch, B.P., Schmitt-Kopplin, P., Perdue, E.M., 2008. Natural organic matter and the event horizon of mass spectrometry. Anal. Chem. 80, 8908–8919. https://doi.org/10.1021/ac800464g.

Hockaday, W.C., Purcell, J.M., Marshall, A.G., Baldock, J.A., Hatcher, P.G., 2009. Electrospray and photoionization mass spectrometry for the characterization of organic matter in natural waters: a qualitative assessment. Limnol Oceanogr. Methods 7, 81–95. https://doi.org/10.4319/lom.2009.7.81.

Hou, C., Chen, L., Dong, Y., Yang, Y., Zhang, X., 2022. Unraveling dissolved organic matter in drinking water through integrated ozonation/ceramic membrane and biological activated carbon process using FT-ICR MS. Water Res. 222, 118881 https://doi.org/10.1016/j.watres.2022.118881.

Ikeya, K., Sleighter, R.L., Hatcher, P.G., Watanabe, A., 2012. Compositional Features of Japanese Humic Substances Society Standard Soil Humic and Fulvic Acids by Fourier

Transform Ion Cyclotron Resonance Mass Spectrometry and X-Ray Diffraction Profile Analysis 9.
Iskander, S.M., Zou, S., Brazil, B., Novak, J.T., He, Z., 2017. Energy consumption by forward osmosis treatment of landfill leachate for water recovery. Waste Manag. 63, 284–291. https://doi.org/10.1016/j.wasman.2017.03.026.
Iskander, S.M., Zhao, R., Pathak, A., Gupta, A., Pruden, A., Novak, J.T., He, Z., 2018. A review of landfill leachate induced ultraviolet quenching substances: sources, characteristics, and treatment. Water Res. 145, 297–311. https://doi.org/10.1016/j.watres.2018.08.035.
Jafari, N.H., Stark, T.D., Thalhamer, T., 2017a. Progression of elevated temperatures in municipal solid waste landfills. J. Geotech. Geoenviron. Eng. 143, 05017004 https://doi.org/10.1061/(ASCE)GT.1943-5606.0001683.
Jafari, N.H., Stark, T.D., Thalhamer, T., 2017b. Spatial and temporal characteristics of elevated temperatures in municipal solid waste landfills. Waste Manag. 59, 286–301. https://doi.org/10.1016/j.wasman.2016.10.052.
Jiménez-González, M.A., Almendros, G., Waggoner, D.C., Álvarez, A.M., Hatcher, P.G., 2020. Assessment of the molecular composition of humic acid as an indicator of soil carbon levels by ultra-high-resolution mass spectrometric analysis. Org. Geochem. 143, 104012 https://doi.org/10.1016/j.orggeochem.2020.104012.
Kang, K.-H., Shin, H.S., Park, H., 2002. Characterization of humic substances present in landfill leachates with different landfill ages and its implications. Water Res. 36, 4023–4032. https://doi.org/10.1016/S0043-1354(02)00114-8.
Kellerman, A., Dittmar, T., Kothawala, D., et al., 2014. Chemodiversity of dissolved organic matter in lakes driven by climate and hydrology. Nat. Commun. 5, 3804. https://doi.org/10.1038/ncomms4804.
Kurniawan, T.A., Lo, W.H., Chan, G.Y.S., 2006. Physico-chemical treatments for removal of recalcitrant contaminants from landfill leachate. J. Hazard Mater. 129, 80–100. https://doi.org/10.1016/j.jhazmat.2005.08.010.
Lee, W.S., Chua, A.S.M., Yeoh, H.K., Ngoh, G.C., 2014. A review of the production and applications of waste-derived volatile fatty acids. Chem. Eng. J. 235, 83–99. https://doi.org/10.1016/j.cej.2013.09.002.
Li, Y., Wang, S., Zhang, L., Zhao, H., Jiao, L., Zhao, Y., He, X., 2014. Composition and spectroscopic characteristics of dissolved organic matter extracted from the sediment of Erhai Lake in China. J. Soils Sediments 14, 1599–1611. https://doi.org/10.1007/S11368-014-0916-2.
Liberatore, Hannah K., Danielle, C., Westerman, Joshua M. Allen, Michael, J. Plewa, Elizabeth, D. Wagner, McKenna, Amy M., Weisbrod, Chad R., et al., 2020. High-resolution mass spectrometry identification of novel surfactant-derived sulfur-containing disinfection byproducts from gas extraction wastewater. Environ. Sci. Technol. 54 (15), 9374–9386. https://doi.org/10.1021/acs.est.0c01997.
Martin, J.W., Stark, T.D., Thalhamer, T., Gerbasi-Graf, G.T., Gortner, R.E., 2013. Detection of aluminum waste reactions and waste fires. Journal of Hazardous, Toxic, and Radioactive Waste 17, 164–174. https://doi.org/10.1061/(asce)hz.2153-5515.0000171.
McKenna, A.M., Chacón-Patiño, M.L., Chen, H., Blakney, G.T., Mentink-Vigier, F., Young, R.B., Ippolito, J.A., Borch, T., 2021. Expanding the analytical window for biochar speciation: molecular comparison of solvent extraction and water-soluble fractions of biochar by FT-ICR mass spectrometry. Anal. Chem. 93 (46), 15365–15372. https://doi.org/10.1021/acs.analchem.1c03058.
Mor, S., Ravindra, K., Dahiya, R.P., Chandra, A., 2006. Leachate characterization and assessment of groundwater pollution near municipal solid waste landfill site. Environ. Monit. Assess. 118, 435–456. https://doi.org/10.1007/s10661-006-1505-7.
Narode, A., Pour-Ghaz, M., Ducoste, J.J., Barlaz, M.A., 2021. Measurement of heat release during hydration and carbonation of ash disposed in landfills using an isothermal calorimeter. Waste Manag. 124, 348–355. https://doi.org/10.1016/j.wasman.2021.02.030.
Ohno, T., He, Z., Sleighter, R.L., Honeycutt, C.W., Hatcher, P.G., 2010. Ultrahigh resolution mass spectrometry and indicator species analysis to identify marker components of soil-and plant biomass-derived organic matter fractions. Environ. Sci. Technol. 44, 8594–8600. https://doi.org/10.1021/es101089t.
Patel, H.V., Brazil, B., Lou, H.H., Jha, M.K., Luster-Teasley, S., Zhao, R., 2021. Evaluation of the effects of chemically enhanced primary treatment on landfill leachate and sewage co-treatment in publicly owned treatment works. J. Water Process Eng. 42, 102116 https://doi.org/10.1016/j.jwpe.2021.102116.
Qi, G., Yue, D., Nie, Y., 2012. Characterization of humic substances in bio-treated municipal solid waste landfill leachate. Front. Environ. Sci. Eng. 6, 711–716. https://doi.org/10.1007/s11783-012-0421-z.
Rivas-Ubach, A., Liu, Y., Bianchi, T.S., Tolić, N., Jansson, C., Pasa-Tolic, L., 2018. Moving beyond the van Krevelen diagram: a new stoichiometric approach for compound classification in organisms. Anal. Chem. 90, 6152–6160. https://doi.org/10.1021/acs.analchem.8b00529.
Roth, H.K., Borch, T., Young, R.B., Bahureksa, W., Blakney, G.T., Nelson, A.R., Wilkins, M.J., McKenna, A.M., 2022. Enhanced speciation of pyrogenic organic matter from wildfires enabled by 21 T FT-ICR mass spectrometry. Anal. Chem. 94 (6), 2973–2980. https://doi.org/10.1021/acs.analchem.1c05018.
Schmidt, M., Torn, M., Abiven, S., et al., 2011. Persistence of soil organic matter as an ecosystem property. Nature 478, 49–56. https://doi.org/10.1038/nature10386.
Schupp, S., De la Cruz, F.B., Cheng, Q., Call, D.F., Barlaz, M.A., 2021. Evaluation of the temperature range for biological activity in landfills experiencing elevated temperatures. ACS EST Eng 1, 216–227. https://doi.org/10.1021/acsestengg.0c00064.
Sleighter, R.L., Hatcher, P.G., 2007. The application of electrospray ionization coupled to ultrahigh resolution mass spectrometry for the molecular characterization of natural organic matter. J. Mass Spectrom. 42, 559–574. https://doi.org/10.1002/jms.1221.
Smith, D.F., Podgorski, D.C., Rodgers, R.P., Blakney, G.T., Hendrickson, C.L., 2018. 21 tesla FT-ICR mass spectrometer for ultrahigh-resolution analysis of complex organic mixtures. Anal. Chem. 90 (3), 2041–2047. https://doi.org/10.1021/acs.analchem.7b04159.
Stark, T.D., Martin, J.W., Gerbasi, G.T., Thalhamer, T., Gortner, R.E., 2012. Aluminum waste reaction indicators in a municipal solid waste landfill. J. Geotech. Geoenviron. Eng. 138, 252–261. https://doi.org/10.1061/(ASCE)GT.1943-5606.0000581.
Steelink, C., 1985. Implications of Elemental Characteristics of Humic Substances. Humic Subst. Soil Sediment Water.
Tatsi, A.A., Zouboulis, A.I., 2002. A field investigation of the quantity and quality of leachate from a municipal solid waste landfill in a Mediterranean climate (Thessaloniki, Greece). Adv. Environ. Res. 6, 207–219. https://doi.org/10.1016/S1093-0191(01)00052-1.
US EPA, 2020. Advancing Sustainable Materials Management: 2018 Fact Sheet Assessing Trends in Materials Generation and Management in the United States. Washington DC.
Valencia, S., Marín, J.M., Restrepo, G., Frimmel, F.H., 2013. Evaluations of the TiO2/simulated solar UV degradations of XAD fractions of natural organic matter from a bog lake using size-exclusion chromatography. Water Res. 47, 5130–5138. https://doi.org/10.1016/j.watres.2013.05.053.
Wang, H., Wang, Y. nan, Li, X., Sun, Y., Wu, H., Chen, D., 2016. Removal of humic substances from reverse osmosis (RO) and nanofiltration (NF) concentrated leachate using continuously ozone generation-reaction treatment equipment. Waste Manag. 56, 271–279. https://doi.org/10.1016/j.wasman.2016.07.040.
Weishaar, J.L., Aiken, G.R., Bergamaschi, B.A., Fram, M.S., Fujii, R., Mopper, K., 2003. Evaluation of specific ultraviolet absorbance as an indicator of the chemical composition and reactivity of dissolved organic carbon. Environ. Sci. Technol. 37, 4702–4708. https://doi.org/10.1021/es030360x.
Wen, D., Ordonez, D., McKenna, A., Chang, N.B., 2020. Fate and transport processes of nitrogen in biosorption activated media for stormwater treatment at varying field conditions of a roadside linear ditch. Environ. Res. 181, 108915 https://doi.org/10.1016/j.envres.2019.108915.
Young, R.B., Pica, N.E., Sharifan, H., Chen, H., Roth, H.K., Blakney, G.T., Borch, T., Higgins, C.P., Kornuc, J.J., McKenna, A.M., Blotevogel, J., 2022. PFAS analysis with ultrahigh resolution 21T FT-ICR MS: suspect and nontargeted screening with unrivaled mass resolving power and accuracy. Environ. Sci. Technol. 56 (4), 2455–2465. https://doi.org/10.1021/acs.est.1c08143.
Yu, W., 2013. Leachate Management in the Aftercare Period of Municipal Waste Landfills at. Finland, Espoo.
Yuan, Q., Jia, H., Poveda, M., 2016. Study on the effect of landfill leachate on nutrient removal from municipal wastewater. J. Environ. Sci. (China) 43, 153–158. https://doi.org/10.1016/j.jes.2015.10.023.
Yuan, Z., He, C., Shi, Q., Xu, C., Li, Z., Wang, C., Zhao, H., Ni, J., 2017. Molecular insights into the transformation of dissolved organic matter in landfill leachate concentrate during biodegradation and coagulation processes using ESI FT-ICR MS. Environ. Sci. Technol. 51, 8110–8118. https://doi.org/10.1021/acs.est.7b02194.
Yuan, Y., Hu, X., Chen, H., Zhou, Y., Zhou, Y., Wang, D., 2019. Advances in enhanced volatile fatty acid production from anaerobic fermentation of waste activated sludge. Sci. Total Environ. 694, 133741 https://doi.org/10.1016/j.scitotenv.2019.133741.
Zhang, Q.Q., Tian, B.H., Zhang, X., Ghulam, A., Fang, C.R., He, R., 2013. Investigation on characteristics of leachate and concentrated leachate in three landfill leachate treatment plants. Waste Manag. 33, 2277–2286. https://doi.org/10.1016/j.wasman.2013.07.021.
Zhao, R., Gupta, A., Novak, J.T., Goldsmith, C.D., Driskill, N., 2013. Characterization and treatment of organic constituents in landfill leachates that influence the UV disinfection in the publicly owned treatment works (POTWs). J. Hazard Mater. 1 (9), 258–259. https://doi.org/10.1016/j.jhazmat.2013.04.026.